ACS OMEGA

http://pubs.acs.org/journal/acsodf

Article

Tunneling Magnetoresistance Transition and Highly Sensitive Pressure Sensors Based on Magnetic Tunnel Junctions with a Black Phosphorus Barrier

Henan Fang,* Qian Li, Mingwen Xiao,* and Yan Liu

Cite This: *ACS Omega* 2022, 7, 20666–20672

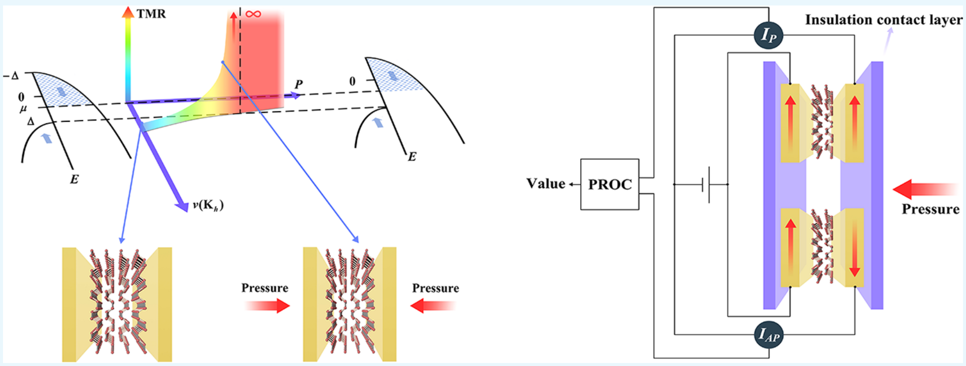

ABSTRACT: Black phosphorus is a promising material to serve as a barrier for magnetic tunnel junctions (MTJs) due to weak van der Waals interlayer interactions. In particular, the special band features of black phosphorus may endow intriguing physical characteristics. Here we study theoretically the effect of band gap tunability of black phosphorus on the MTJs with the black phosphorus barrier. It is found that the tunneling magnetoresistance (TMR) may transition from a finite value to infinity owing to the variation in the band gap of black phosphorus. Combined with the latest experimental results of the pressure-induced band gap tunability, we further investigate the pressure effect of TMR in the MTJs with a black phosphorus barrier. The calculations show that the pressure sensitivity can be quite high under appropriate parameters. Physically, the high sensitivity originates from the TMR transition phenomenon. To take advantage of the high pressure sensitivity, we propose and design a detailed structure of highly sensitive pressure sensors based on MTJs with a black phosphorus barrier, whose working mechanism is basically different from that of convential pressure sensors. The present pressure sensors possess four advantages and benefits: (1) high sensitivity, (2) good anti-interference, (3) high spatial resolution, and (4) fast response speed. Our study may advance new research areas for both the MTJs and pressure sensors.

INTRODUCTION

Black phosphorus is one type of two-dimensional semiconductor that has received tremendous attention owing to its two-dimensionality and the availability of advanced characterization techniques.[1] For practical applications, black phosphorus has great potential in field effect transistors, photodetectors, batteries, etc.[1] In the field of spintronics, weak van der Waals interlayer interactions make it possible for black phosphorus to serve as a barrier for magnetic tunnel junctions (MTJs). Up to now, research on MTJs with a phosphorus barrier has been rarely addressed.[2] In particular, the band gap tunability of black phosphorus, which may play a key role in tunneling magnetoresistance (TMR), has never been adequately considered.

The band gap tunability of black phosphorus mainly manifests in two ways: thickness (layer) dependence and pressure dependence. On one hand, the band gap of black phosphorus is highly dependent on the thickness.[1,3−5] For monolayer black phosphorus, the band gap is about 2 eV,[1,3,5,6] while for bulk black phosphorus, the band gap is only about 0.3 eV.[1,3,5,7] On the other hand, quite recently, S. Huang et al. investigated experimentally the pressure effect on the electronic structure of black phosphorus.[8] They found that the relative changes in band gap versus pressure depend on the number of layers of black phosphorus, which can be expressed as follows:

Received: February 5, 2022
Accepted: May 30, 2022
Published: June 9, 2022

https://doi.org/10.1021/acsomega.2c00748
ACS Omega 2022, 7, 20666–20672

$$\triangle E_g^N(P) = aP - \frac{\gamma_0}{2}\left(\sqrt{1+\frac{P}{P_{coh}}} - 1\right)\cos\left(\frac{1}{N+1}\pi\right) \quad (1)$$

where P is the magnitude of the pressure, N is the number of the layers, a is the changing rate, γ_0 is the difference of overlapping integrals for the conduction band and valence band under 0 GPa, and P_{coh} is the cohesive pressure. In ref 8, both the experiments and the derivation of eq 1 are irrelevant to the substrate. That is, eq 1 represents the physical properties of black phosphorus alone. In addition, it is worth noting that eq 1 is valid only for the case where the thickness of black phosphorus is not greater than 50 nm. This is because, for bulk black phosphorus, there is additional in-plane compressive strain besides the normal strain.[8] The above band gap tunability may endow novel characteristics to MTJs with a black phosphorus barrier, and more importantly, those characteristics could possibly lead to new applications.

Here we investigate theoretically the effect of band gap tunability on MTJs with a black phosphorus barrier. As can be seen in the following, the band gap tunability may result in a TMR transition phenomenon. Furthermore, through utilizing the TMR transition, we propose and design a kind of highly sensitive pressure sensor, and its working mechanism is entirely different from that of conventional pressure sensors. Next, to help readers understand the TMR transition phenomenon, we shall briefly illustrate the physical background.

THEORETICAL BACKGROUND

In conventional theories, e.g., Jullière's model and Slonczewski's model,[9,10] MTJs with half-metallic electrodes will obtain infinite TMR near zero bias and low temperature. However, the experimental TMR in such MTJs is far from infinity,[11,12] which contradicts conventional theories. In other words, the conventional theories are inapplicable to experiments. Recently, a new spintronic theory was developed by us to handle MTJs with single-crystal barriers.[13] The theory is founded on traditional optical scattering theory.[14] Within it, the barrier is treated as a diffraction grating that will result in strong coherence to the tunneling electrons. So far, the theory has successfully explained almost all the important effects in MgO-based MTJs, including the barrier thickness effect,[13] temperature effect,[15] bias effect,[16] etc. In particular, the theory works well when it is applied to MTJs with half-metallic electrodes, and it can clarify clearly the physical mechanism for the contradiction between the conventional theories and experiments.[17] Meanwhile, the theory shows that, for MTJs with half-metallic electrodes, the TMR can be finite or infinite, which depends on the relationship between the Fourier transformation of the atomic potential of the barrier $\nu(\mathbf{K}_h)$, the chemical potential of the electrodes μ, and half of the exchange splitting of the electrodes Δ. At zero bias voltage limit, if $\nu(\mathbf{K}_h) > \Delta - \mu$, the TMR will be finite, and vice versa. In physics, the parameter $\nu(\mathbf{K}_h)$ should be approximately proportional to the band gap of the barrier.[13,14] As such, if the band gap of the barrier is tunable within a wide range, it may occur that, in the tunable range of the band gap, there is a critical point corresponding to $\nu(\mathbf{K}_h) = \Delta - \mu$. Of course, on one side of the critical point, $\nu(\mathbf{K}_h) > \Delta - \mu$, and on the other side, $\nu(\mathbf{K}_h) < \Delta - \mu$. In this case, the TMR can transition from a finite value to infinity just around the critical point even if the material of the barrier remains unchanged.

As pointed out above, the band gap of black phosphorus is highly dependent on the thickness. The wide range of band gap modulation suggests that black phosphorus may be a good candidate as a barrier for realizing the scenario proposed above, i.e., the TMR can transition from a finite value to infinity in MTJs consisting of a black phosphorus barrier with different thicknesses and half-metallic electrodes. The physical picture is illustrated schematically in Figure 1 where the z-axes

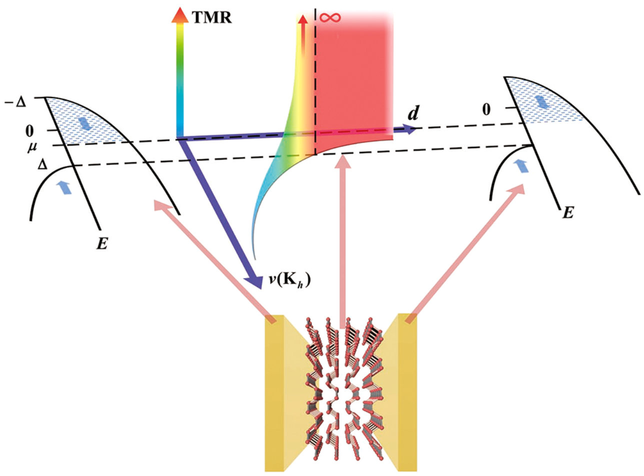

Figure 1. Diagram for the thickness effect in MTJs with a black phosphorus barrier and half-metallic electrodes at zero bias limit.

of spin for the two ferromagnetic electrodes are respectively chosen as their own. As shown in Figure 1, the TMR tends to infinity at a certain thickness which will be called "critical thickness" in the following. This means that the TMR is extremely sensitive to a variation in barrier thickness when the barrier thickness is slightly less than the critical thickness. In physics, that is because the critical thickness just corresponds to the critical equation $\nu(\mathbf{K}_h) = \Delta - \mu$, as can been seen in Figure 1.

Let us now turn to the pressure effect. According to ref 8, when $N \geq 5$, the band gap of black phosphorus will decrease monotonically with pressure in the range of 0 GPa to 1 GPa, and the change is a few tens of meV/GPa. Considering the case that when the MTJs are without pressure, $\nu(\mathbf{K}_h)$ is slightly larger than $\Delta - \mu$, and then a pressure is applied to the MTJs. In such a case, $\nu(\mathbf{K}_h)$ will decrease with the pressure and further tend to $\Delta - \mu$. Accordingly, the TMR will be extremely sensitive to the pressure, and the principle is essentially the same as the thickness effect. This provides a possible working mechanism for the highly sensitive pressure sensors based on MTJs with a black phosphorus barrier, which is illustrated schematically in Figure 2.

In the following, we shall calculate comprehensively the thickness effect and pressure effect of the MTJs with a black phosphorus barrier (the theoretical model used for the calculations and the definition of TMR can be found in the Supporting Information). According to the calculations, we designed in detail the device prototype of the highly sensitive pressure sensors and discuss the advantages and benefits of it.

RESULTS AND DISCUSSION

The parameters in the calculations are set as follows. As stated in Theoretical Background, the band gap E_g of black phosphorus is highly dependent on the thickness. Until now,

https://doi.org/10.1021/acsomega.2c00748
ACS Omega 2022, 7, 20666−20672

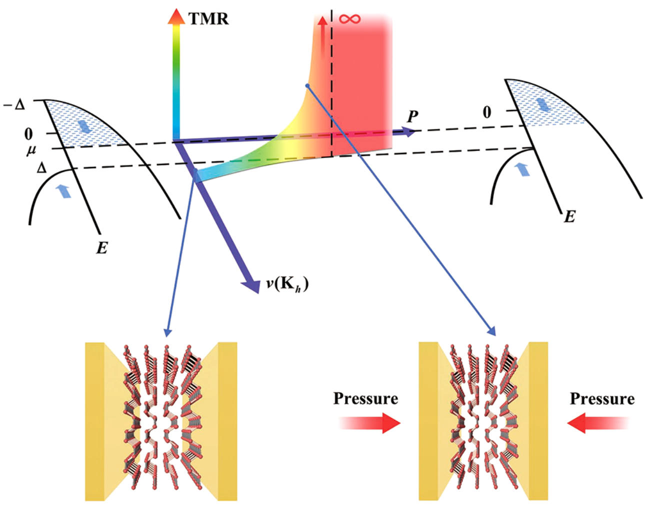

Figure 2. Diagram for the pressure effect in MTJs with a black phosphorus barrier and half-metallic electrodes at zero bias limit.

there has been no unified expression of the dependence.[4,5] Here we adopt the expression of ref 5:

$$E_g = A\ \exp(-BN)/N^C + D \tag{2}$$

where A = 1.71 eV, B = 0.17, C = 0.73, and D = 0.40 eV. Because $\nu(\mathbf{K}_h)$ should be approximately proportional to the band gap,[13,14] we assume that the thickness dependence of $\nu(\mathbf{K}_h)$ is the same as E_g. Considering that the thickness of monolayer black phosphorus is 0.524 nm,[18] we shall set

$$\nu(\mathbf{K}_h) = 3.42\ \text{eV}\ \exp(-0.17d/0.524\ \text{nm})/(d/0.524\ \text{nm})^{0.73} + 0.8\ \text{eV} \tag{3}$$

where d is the thickness of the black phosphorus barrier. As for the pressure effect, according to ref 8, the parameters in eq 1 are set as follows: a = 0.18 eV/GPa, γ_0 = 1.76 eV, P_{coh} = 1.4 GPa. In addition, because the magnitude of the intralayer primitive translational vector c = 4.3763 Å,[18] the magnitude of the intralayer reciprocal lattice vector $K_h = 2\pi/c = 1.436 \times 10^{10}$ m^{-1}.

Thickness Effect of the TMR in MTJs with a Black Phosphorus Barrier. First, we investigated the thickness dependence of conductances and TMR under different bias voltages. The theoretical results are depicted in Figure 3 where the chemical potential μ is 3 eV, half of the exchange splitting Δ is 5 eV, and the bias V_0 is set sequentially as 0, 0.1, 0.5, and 1 V. As shown in Figure 3a, G_P varies nonmonotonically with the barrier thickness, which originates from the interference among the diffracted waves, as pointed out in ref 13. Unlike G_P, G_{AP} first decreases with the barrier thickness and tends to zero at a certain thickness, as depicted in Figure 3b. It can be explained as follows: according to eq 3, $\nu(\mathbf{K}_h)$ decreases monotonously with barrier thickness. Physically, the smaller the $\nu(\mathbf{K}_h)$, the less energy the tunneling electrons will acquire. Therefore, the decreasing $\nu(\mathbf{K}_h)$ reduces the number of tunneling electrons having sufficient energy to transit from the spin-up band into the spin-down band. For the case of zero bias limit, as the barrier thickness increases, there will be a critical thickness ($d \approx 1.26$ nm) that corresponds to $\nu(\mathbf{K}_h) = \Delta - \mu$. At this critical thickness, G_{AP} tends to zero because the energy $\nu(\mathbf{K}_h)$ will be insufficient for the incident spin-up electrons to transit into the spin-down band. For the finite bias case, the larger the bias voltage, the greater the critical thickness. This is because the critical thickness corresponds to $\nu(\mathbf{K}_h) = \Delta - \mu - eV_0$ now, which is illustrated schematically in Figure 4. From Figure 4, it

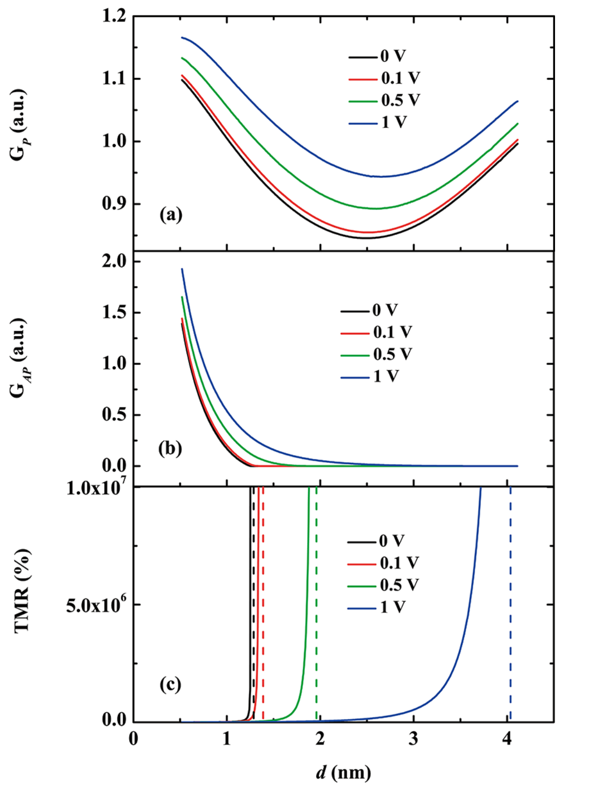

Figure 3. (a) G_P, (b) G_{AP}, and (c) TMR as functions of barrier thicknesses under different bias voltages V_0 = 0 V, 0.1 V, 0.5 V, and 1 V. Here the dashed lines denote the critical barrier thicknesses.

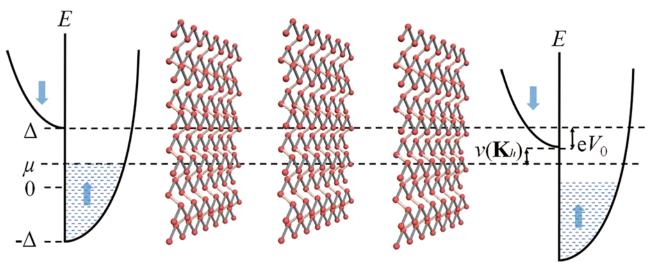

Figure 4. An illustration of the potential of the MTJs at finite bias. Here the $\nu(\mathbf{K}_h)$ corresponds to the critical equation $\nu(\mathbf{K}_h) = \Delta - \mu - eV_0$.

can be seen that larger bias can reduce the energy required for the spin-up electrons to transit into the spin-down band, i.e., smaller $\nu(\mathbf{K}_h)$ is needed. According to eq 3, the critical thickness will be greater. Consequently, the TMR will achieve a transition from a finite value to infinity around those critical thicknesses, as shown in Figure 3c. This is just the critical thickness phenomenon presented in Figure 1.

Second, we shall study the thickness dependence of conductances and TMR under different half of the exchange splittings. The theoretical results are depicted in Figure 5 where the chemical potential μ is 3 eV, the bias is 0.1 V, and the half of the exchange splitting Δ is set sequentially as 4, 5, and 6 eV. As can be seen in Figure 5b,c, the critical thickness decreases with the half of the exchange splitting Δ. This can be easily understood: according to the critical equation $\nu(\mathbf{K}_h) = \Delta$

https://doi.org/10.1021/acsomega.2c00748
ACS Omega 2022, 7, 20666−20672

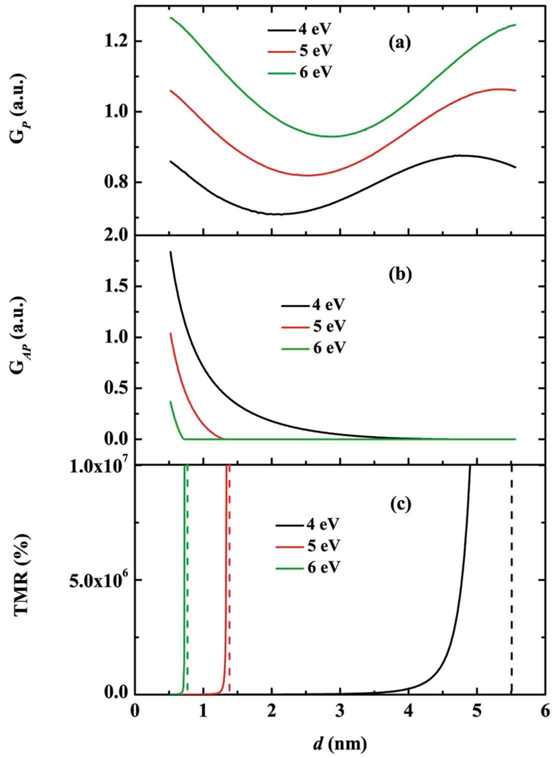

Figure 5. (a) G_P, (b) G_{AP}, and (c) TMR as functions of barrier thicknesses under different half of the exchange splittings Δ = 4, 5, and 6 eV. Here the dashed lines denote the critical barrier thicknesses.

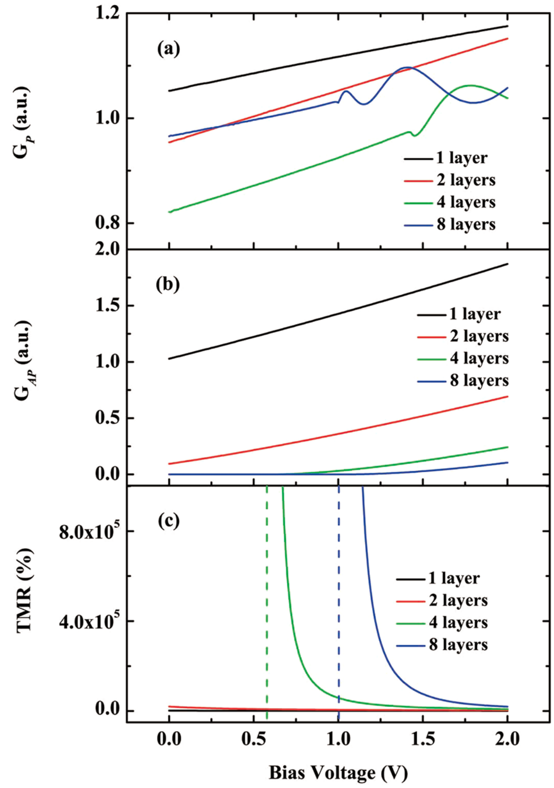

Figure 6. (a) G_P, (b) G_{AP}, and (c) TMR as functions of bias voltage under different numbers of layers of the black phosphorus barrier N = 1, 2, 4, and 8. Here the dashed lines denote the critical bias voltage.

$-\ \mu - eV_0$, when Δ increases, the $\nu(\mathbf{K}_h)$ corresponding to the critical thickness increases as well. From eq 3, it can be known that the critical thickness will decrease with Δ.

As indicated in Figures 3 and 5, the critical thicknesses can be regulated by both the bias voltage and the parameters of the half-metallic ferromagnetic electrodes, which entirely derives from the critical equation $\nu(\mathbf{K}_h) = \Delta - \mu - eV_0$. In the critical thickness phenomenon, the right side of the critical equation remains unchanged, and the left side of the critical equation, i.e., $\nu(\mathbf{K}_h)$, varies to cross the critical point. Conversely, if the left side of the critical equation remains unchanged, and the right side of the critical equation, i.e., the bias voltage V_0 or the half of the exchange splitting Δ, varies to cross the critical point, there will also appear a critical phenomenon. In practical applications, the bias voltage is more easily altered than the parameters of the half-metallic ferromagnetic electrodes. That is to say, the critical bias phenomenon can be easier to be observed. Thereupon, we will discuss the bias dependence of conductances and TMR under different numbers of layers of the black phosphorus barrier. The theoretical results are depicted in Figure 6 where the chemical potential μ is 3 eV, the half of the exchange splitting Δ is 5 eV, and the number of the layers of the black phosphorus barrier N is set sequentially as 1, 2, 4, and 8. As shown in Figure 6a, when N = 4 and N = 8, there are critical points located around 1.43 and 1 V, respectively, for G_P. On the right side of the critical points, G_P oscillates with the bias voltage, whereas on the left side G_P does not. It can be explained as follows: in the present case, the oscillation of G_P originates from the oscillation term of $\cos[(p_+^z - p_-^z)d]$ that belongs to the channel of $T_{\uparrow\uparrow}$. It can be deduced from eq 3 of the Supporting Information that, on the right side of the critical points, p_-^z will be real in all integral regions for the channel of $T_{\uparrow\uparrow}$; on the left side of the critical points, p_-^z will be imaginary in some integral regions, which will damage the oscillation property of $\cos[(p_+^z - p_-^z)d]$. More importantly, it can be seen from Figure 6c that, for N = 4 and N = 8, TMR transitions from a finite value to infinity around V_0 = 0.57 V and V_0 = 1 V, respectively. The above two values of V_0 meet the critical equation $\nu(\mathbf{K}_h) = \Delta - \mu - eV_0$, and this is just the critical bias phenomenon mentioned above. For the cases of N = 1 and N = 2, $\Delta - \mu - eV_0$ is always smaller than $\nu(\mathbf{K}_h)$, so the critical bias phenomenon will not happen. In other words, the critical phenomenon only can happen when critical equation $\nu(\mathbf{K}_h) = \Delta - \mu - eV_0$ is met in the variable range.

Pressure Effect of the TMR in MTJs with Black Phosphorus Barrier. As examples, we calculate, respectively, the pressure effect of the TMR for three different thicknesses of the black phosphorus barrier, i.e., N = 5, N = 10, and N = 20. The parameters are chosen to satisfy the condition that, when the MTJs are without pressure, $\nu(\mathbf{K}_h)$ is slightly larger than $\Delta - \mu - eV_0$. For the case of N = 5, μ = 3 eV, Δ = 4.2 eV, and eV_0 = 70 meV, for the case of N = 10, μ = 3 eV, Δ = 3.8 eV, and eV_0 = 50 meV, and for the case of N = 20, μ = 3 eV, Δ = 3.7 eV, and eV_0 = 70 meV. The theoretical results are depicted in Figure 7 where the vertical is exponential type. As shown in Figure 7, for all three cases, the TMR increases with the pressure even more rapidly than the exponential form. This is because, according to eq 1, the band gaps of black phosphorus for these three thicknesses all decrease monotonically with pressure within the range 0−1 GPa. In this sense, the monotonically decreasing range of the pressure−band gap curve should be the theoretical range of detection. From eq 1, it can be derived that the greater the number of layers, the

https://doi.org/10.1021/acsomega.2c00748
ACS Omega 2022, 7, 20666−20672

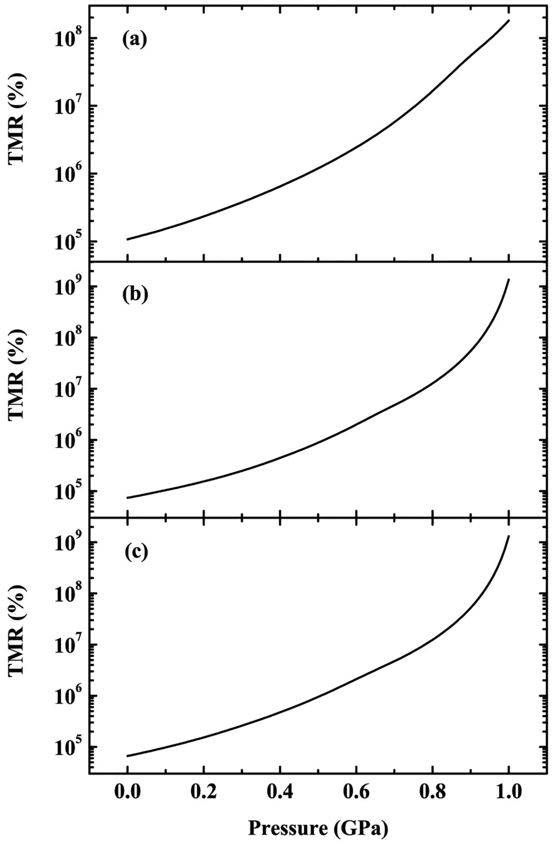

Figure 7. TMR as functions of pressure under different numbers of layers of a black phosphorus barrier: (a)N = 5, (b) N = 10, and (c) N = 20.

larger the theoretical range of detection: for the number of layers N = 5, the theoretical range of detection is about 0−1.8 GPa; for N = 10, the theoretical range of detection is about 0−2.5 GPa; for N = 20, the theoretical range of detection is about 0−2.8 GPa. It is worth noting that the range of the experimental data in ref 8 only includes 0−2.5 GPa, and therefore the theoretical range of detection for N = 20 is only theoretically derived from eq 1. In the present case, the sensitivity can be defined as $(\Delta TMR/TMR_0)/\Delta P$, where ΔTMR is the change in TMR, TMR_0 is the TMR under no pressure, and ΔP is the change in pressure. It can be deduced from Figure 7 that the highest sensitivity can reach 8.53×10^2 MPa^{-1} at 1 GPa for the case of N = 20. Such high sensitivity originates from the TMR transition at the critical point, as displayed in Figure 2. In principle, the present pressure sensors can reach arbitrary high sensitivity if the measuring range can be sacrificed. This is because, at the critical point of the TMR transition, the TMR has an infinite derivative as well as sensitivity. In theory, we can let $\Delta - \mu - eV_0$ tend to $v(\mathbf{K}_h)$ infinitely, which means that the sensitivity can be arbitrarily high. The above results declare that the MTJs with a black phosphorus barrier indeed can be a potential system as highly sensitive pressure sensors.

Design of Highly Sensitive Pressure Sensors. Pressure sensors have a wide range of applications, such as transportation, automobile industries, and the medical field.[19] They constitute an important component of the field of microelectromechanical systems (MEMS) and have the highest market share among all kinds of MEMS sensors.[20] The performance of pressure sensors can be assessed from many aspects; nevertheless, there is no doubt that the sensitivity is a vital parameter.[21] In particular, pressure sensors with high sensitivity are urgently needed in nanotechnology. When the sensitivity is high, good anti-interference, high spatial resolution, and fast response speed are usually necessary. Therefore, the requirements of high sensitivity, good anti-interference, high spatial resolution, and fast response speed are goals for the development of pressure sensors. Unfortunately, conventional types of pressure sensors (e.g., piezoresistive-type sensors and capacitance-type sensors) cannot completely meet the above requirements.[22] This suggests that novel sensing technology should be proposed to improve the corresponding performances.

On the other hand, the applications of MTJs are mainly focused on magnetic memory storage cells and magnetic field sensors. Besides the above familiar applications, M. Löhndorfa et al. developed a type of pressure sensor based on MTJs.[22,23] Its working mechanism utilizes the inverse magnetostrictive effect (Villary effect), i.e., the shear pressure leads to a change in the magnetization direction of the free layer. In addition, the pressure sensitivity is described by the gauge factor: GF = $(\Delta R/R)/\Delta\varepsilon$, where $\Delta R/R$ is the relative change in resistance and $\Delta\varepsilon$ is the relative change in strain. Subsequently, a certain amount of research effort has been devoted to improve the performances, especially the GF, of such pressure sensors.[24−27] These works have initiated a new research direction for both MTJs and pressure sensors and indicate that the pressure sensors based on MTJs have great potential to satisfy the requirements mentioned above. However, owing to the working mechanism, this type of pressure sensor can only measure the shear pressure and is not applicable to the measurement of normal pressure. That confines the applications to certain fields.

Therefore, a new kind of MTJ-based pressure sensor which can measure the normal pressure is needed. The present calculations of the pressure effect demonstrate that the MTJ with a black phosphorus barrier is a good candidate to satisfy this need. Different from previous MTJ-based pressure sensors, the working mechanism now is the TMR transition due to the pressure effect of black phosphorus. According to ref 8, the pressure-induced variation of band gap derives from the decrease of the interlayer distance. In other words, the pressure in the normal direction leads to the variation of TMR. Therefore, the pressure sensors based on MTJs with a black phosphorus barrier are suitable for measuring the normal pressure. To facilitate the practical application, a detailed structure of the device was designed, which is displayed in Figure 8. It can be seen from Figure 8 that two MTJs with different magnetization configurations are in parallel connection to the output parallel current and antiparallel current, respectively. Such a design has two advantages: (1) the parallel current I_P and antiparallel current I_{AP} can be simultaneously obtained, which can improve the response speed. (2) If noise exists, it can only influence the magnitudes of I_P and I_{AP} but has no influence on the magnitude of TMR. In other words, the present pressure sensors have good anti-interference. In addition, nanometer scale MTJs can lead to miniaturized pressure sensors with high spatial resolution.[22] Including the high sensitivity mentioned above, the present pressure sensors possess four advantages and benefits: (1) high sensitivity, (2) good anti-interference, (3) high spatial resolution, and (4) fast response speed. Furthermore, the completely new working

https://doi.org/10.1021/acsomega.2c00748
ACS Omega 2022, 7, 20666−20672

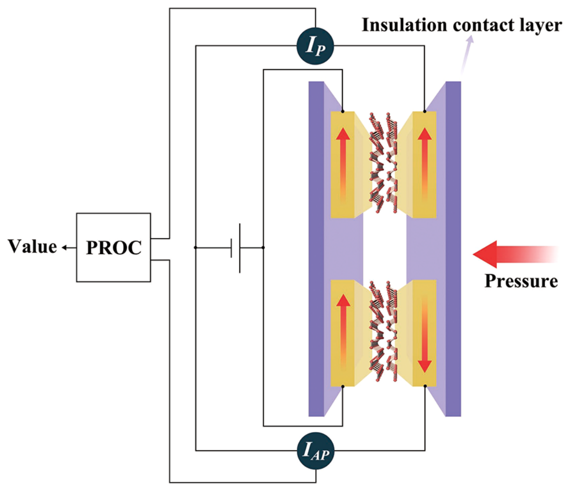

Figure 8. Design diagram of the highly sensitive pressure sensor based on MTJs with a black phosphorus barrier.

mechanism may lead to a novel research area for both the pressure sensors and the MTJs.

CONCLUSIONS

In this paper, we have studied the thickness effect and pressure effect of the MTJs with a black phosphorus barrier. We found a TMR transition phenomenon: the TMR will transition from a finite value to infinity around the critical thickness. The critical thickness can be regulated by both the bias voltage and half of the exchange splitting of electrodes. For the range of numbers of the black phosphorus layers, $5 \leq N \leq 20$, the TMR increases with the pressure more rapidly than the exponential form under appropriate parameters, and the sensitivity can be as high as 8.53×10^2 MPa^{-1} at 1 GPa for the case of $N = 20$. Such high sensitivity originates from the TMR transition at the critical point. Furthermore, according to the calculations of the pressure effect, we designed in detail the structure of the highly sensitive pressure sensors, and the design diagram is given. The advantages and benefits of the present pressure sensors were discussed. Finally, the present work should not be confined to MTJs with a black phosphorus barrier. It can be extended to MTJs with other band-tunable barriers, such as MoS_2.[28,29]

ASSOCIATED CONTENT

Supporting Information

The Supporting Information is available free of charge at https://pubs.acs.org/doi/10.1021/acsomega.2c00748.

Theoretical model for magnetic tunnel junctions with a single-crystal barrier (PDF)

AUTHOR INFORMATION

Corresponding Authors

Henan Fang − *College of Electronic and Optical Engineering, Nanjing University of Posts and Telecommunications, Nanjing 210023, China*; orcid.org/0000-0002-7693-573X; Email: fanghn@njupt.edu.cn

Mingwen Xiao − *Department of Physics, Nanjing University, Nanjing 210093, China*; orcid.org/0000-0002-1005-3179; Email: xmw@nju.edu.cn

Authors

Qian Li − *College of Electronic and Optical Engineering, Nanjing University of Posts and Telecommunications, Nanjing 210023, China*

Yan Liu − *College of Electronic and Optical Engineering, Nanjing University of Posts and Telecommunications, Nanjing 210023, China*

Complete contact information is available at: https://pubs.acs.org/10.1021/acsomega.2c00748

Notes

The authors declare no competing financial interest.

ACKNOWLEDGMENTS

This work is supported by the National Natural Science Foundation of China (11704197) and the Natural Science Foundation of Nanjing University of Posts and Telecommunications (NY220184, NY221066).

REFERENCES

(1) Eswaraiah, V.; Zeng, Q. S.; Long, Y.; Liu, Z. Black phosphorus nanosheets: synthesis, characterization and applications. *Small* **2016**, *12*, 3480−3502.

(2) Chen, M.; Yu, Z.; Xie, Y.; Wang, Y. Spin-polarized quantum transport properties through flexible phosphorene. *Appl. Phys. Lett.* **2016**, *109*, 142409.

(3) Wu, S. X.; Hui, K. S.; Hui, K. N. 2D black phosphorus: from preparation to applications for electrochemical energy storage. *Adv. Sci.* **2018**, *5*, 1700491.

(4) Tran, V.; Soklaski, R.; Liang, Y. F.; Yang, L. Layer-controlled band gap and anisotropic excitons in few-layer black phosphorus. *Phys. Rev. B* **2014**, *89*, 235319.

(5) Rudenko, A. N.; Yuan, S. J.; Katsnelson, M. I. Toward a realistic description of multilayer black phosphorus: From GW approximation to large-scale tight-binding simulations. *Phys. Rev. B* **2015**, *92*, 085419.

(6) Liang, L. B.; Wang, J.; Lin, W. Z.; Sumpter, B. G.; Meunier, V.; Pan, M. H. Electronic bandgap and edge reconstruction in phosphorene materials. *Nano Lett.* **2014**, *14*, 6400−6406.

(7) Keyes, R. W. The electrical properties of black phosphorus. *Phys. Rev.* **1953**, *92*, 580−584.

(8) Huang, S.; Lu, Y.; Wang, F.; Lei, Y.; Song, C.; Zhang, J.; Xing, Q.; Wang, C.; Xie, Y.; Mu, L.; Zhang, G.; Yan, H.; Chen, B.; Yan, H. Layer-dependent pressure effect on the electronic structure of 2D black phosphorus. *Phys. Rev. Lett.* **2021**, *127*, 186401.

(9) Jullière, M. Tunneling between ferromagnetic films. *Phys. Lett.* **1975**, *54A*, 225−226.

(10) Slonczewski, J. C. Conductance and exchange coupling of two ferromagnets seperated by a tunneling barrier. *Phys. Rev. B* **1989**, *39*, 6995−7002.

(11) Ishikawa, T.; Hakamata, S.; Matsuda, K.; Uemura, T.; Yamamoto, M. Fabrication of fully epitaxial $Co_2MnSi/MgO/Co_2MnSi$ magnetic tunnel junctions. *J. Appl. Phys.* **2008**, *103*, 07A919.

(12) Hu, B.; Moges, K.; Honda, Y.; Liu, H.; Uemura, T.; Yamamoto, M.; Inoue, J.; Shirai, M. Temperature dependence of spin-dependent tunneling conductance of magnetic tunnel junctions with half-metallic Co_2MnSi electrodes. *Phys. Rev. B* **2016**, *94*, 094428.

(13) Fang, H. N.; Xiao, M. W.; Rui, W. B.; Du, J.; Tao, Z. K. Magnetic coherent tunnel junctions with periodic grating barrier. *Sci. Rep.* **2016**, *6*, 24300.

(14) Cowley, J. M. *Diffraction Physics*, 3nd ed.; Elsevier: Amsterdam, 1995; pp 170−180.

(15) Fang, H. N.; Xiao, M. W.; Rui, W. B.; Du, J.; Tao, Z. K. K. Effects of temperature on the magnetic tunnel junctions with periodic grating barrier. *J. Magn. Magn. Mater.* **2018**, *465*, 333−338.

(16) Fang, H. N.; Zang, X.; Xiao, M. W.; Zhong, Y. Y.; Tao, Z. K. Oscillations of tunneling magnetoresistance on bias voltage in

magnetic tunnel junctions with periodic grating barrier. *J. Appl. Phys.* **2020**, *127*, 163902.
(17) Fang, H. N.; Xiao, M. W.; Zhong, Y. Y.; Rui, W. B.; Du, J.; Tao, Z. K. Magnetic tunnel junctions consisting of a periodic grating barrier and two half-metallic electrodes. *New J. Phys.* **2019**, *21*, 123006.
(18) Asahina, H.; Shindo, K.; Morita, A. Electronic structure of black phosphorus in self-consistent pseudopotential approach. *J. Phys. Soc. Jpn.* **1982**, *51*, 1193−1199.
(19) Zhao, Y.; Liu, Y.; Li, Y.; Hao, Q. Development and application of resistance strain force sensors. *Sensors* **2020**, *20*, 5826.
(20) Kumar, S. S.; Pant, B. D. Design principles and considerations for the 'ideal' silicon piezoresistive pressure sensor: a focused review. *Microsyst. Technol.* **2014**, *20*, 1213−1247.
(21) Chang, X.; Chen, L.; Chen, J.; Zhu, Y.; Guo, Z. Advances in transparent and stretchable strain sensors. *Adv. Compos. Hybrid Mater.* **2021**, *4*, 435−450.
(22) Löhndorf, M.; Duenas, T.; Tewes, M.; Quandt, E.; Rührig, M.; Wecker, J. Highly sensitive strain sensors based on magnetic tunneling junctions. *Appl. Phys. Lett.* **2002**, *81*, 313−315.
(23) Löhndorf, M.; Dokupil, S.; Bootsmann, M.-T.; Malavé, A.; Rührig, M.; Bär, L.; Quandt, E. Characterization of magnetostrictive TMR pressure sensors by MOKE. *J. Magn. Magn. Mater.* **2007**, *316*, e223−e225.
(24) Meyners, D.; von Hofe, T.; Vieth, M.; Rührig, M.; Schmitt, S.; Quandt, E. Pressure sensor based on magnetic tunnel junctions. *J. Appl. Phys.* **2009**, *105*, 07C914.
(25) Tavassolizadeh, A.; Hayes, P.; Rott, K.; Reiss, G.; Quandt, E.; Meyners, D. Highly strain-sensitive magnetostrictive tunnel magnetoresistance junctions. *J. Magn. Magn. Mater.* **2015**, *384*, 308−313.
(26) Fuji, Y.; Kaji, S.; Hara, M.; Higashi, Y.; Hori, A.; Okamoto, K.; Nagata, T.; Baba, S.; Yuzawa, A.; Otsu, K.; Masunishi, K.; Ono, T.; Fukuzawa, H. Highly sensitive spintronic strain-gauge sensor based on a MgO magnetic tunnel junction with an amorphous CoFeB sensing layer. *Appl. Phys. Lett.* **2018**, *112*, 062405.
(27) Fuji, Y.; Higashi, Y.; Masunishi, K.; Yuzawa, A.; Nagata, T.; Kaji, S.; Okamoto, K.; Baba, S.; Ono, T.; Hara, M. Spin-MEMS microphone integrating a series of magnetic tunnel junctions on a rectangular diaphragm. *J. Appl. Phys.* **2018**, *123*, 163901.
(28) Mak, K. F.; Lee, C.; Hone, J.; Shan, J.; Heinz, T. F. Atomically thin MoS_2: A new direct-gap semiconductor. *Phys. Rev. Lett.* **2010**, *105*, 136805.
(29) Fu, L.; Wan, Y.; Tang, N.; Ding, Y.; Gao, J.; Yu, J.; Guan, H.; Zhang, K.; Wang, W.; Zhang, C.; Shi, J.; Wu, X.; Shi, S.; Ge, W.; Dai, L.; Shen, B. K-Λ crossover transition in the conduction band of monolayer MoS_2 under hydrostatic pressure. *Sci. Adv.* **2017**, *3*, e1700162.

https://doi.org/10.1021/acsomega.2c00748
ACS Omega 2022, 7, 20666−20672